LBL-15823
Preprint

Lawrence Berkeley Laboratory
UNIVERSITY OF CALIFORNIA

EARTH SCIENCES DIVISION

To be published in the International Journal of Rock Mechanics and Mining Sciences

STATIC AND DYNAMIC ELASTIC PROPERTIES OF IGNEOUS AND METAMORPHIC ROCKS FROM THE CANADIAN SHIELD

M.S. King

April 1983

Prepared for the U.S. Department of Energy under Contract DE-AC03-76SF00098

DISCLAIMER

LBL-15823

Static and Dynamic Elastic Properties of Igneous and Metamorphic Rocks from the Canadian Shield

M. S. King*

Department of Geological Sciences
University of Saskatchewan
Saskatoon, Canada, S7N OWO

Accepted for publication in the
International Journal of Rock
Mechanics and Mining Sciences,
v. 20, 1983.

*Now with: Earth Sciences Division
Lawrence Berkeley Laboratory
University of California
Berkeley, CA 94720

INTRODUCTION

Techniques involving the propagation of acoustic or seismic waves are becoming of increasing importance in the characterization of rock masses in mineral exploration, mining operations, site investigations and other engineering applications. Several examples follow of the use of such techniques. Hajnal et al (1983) discuss the seismic characteristics of igneous and metamorphic rocks of the Canadian Shield, with potential applications to mineral exploration and the underground disposal of hazardous wastes. McCann et al (1975) describe the use of cross-hole acoustic measurements to delineate interfaces between homogeneous media, to detect localized, irregular features, and to estimate the degree of fracturing in rock masses. Sjogren et al (1979) discuss correlations between compressional-wave velocities and such rock-mechanics parameters as fracture frequency and rock quality (RQD), with the objective of establishing a seismic classification for rock mass quality. Gladwin and Stacey (1974) and Gladwin (1982) describe the development and use of a cross-hole acoustic stress-inferring device to predict pillar failure in an Australian underground copper mine. McKenzie et al (1982) discuss the use of the same cross-hole acoustic system for characterizing the rock mass at several Australian open-pit and underground mines. King et al (1978) discuss the use of an acoustic borehole logging system for determining rock mass quality, in particular to gauging the extent of blast damage adjacent to underground mine openings in western Canada. West and Grant (1981) describe a similar acoustic borehole logging application to probing the strength of rock ahead of tunnels. Paulsson and King (1980a, 1980b) present preliminary results of cross-hole acoustic monitoring conducted as part of an underground nuclear-waste disposal research study in granite.

The relationships between static and dynamic elastic moduli have been studied by, amongst others, Simmons and Brace (1965), King (1970), Geyer and Myung (1971), Myung and Helander (1972), and Paulsson and King (1980b). These workers have demonstrated that at atmospheric pressure and at low confining stresses the static elastic modulus for dry rocks is generally less than the dynamic. The reason for the difference is ascribed to the presence of microcracks or microfractures which affect the strain of the entire rock specimen during a static measurement more than the propagation characteristics of ultrasonic waves during a dynamic measurement. Where the concentration of microcracks is low, the static elastic modulus for a dry rock approaches the dynamic value.

For water-saturated rocks the case is much more complicated. The static elastic modulus and strength are decreased upon saturation, due to the reduction in free surface energy in the presence of a strongly adsorbed liquid (Boozer et al, 1963). The dynamic elastic modulus increases, however, despite a small concomitant increase in density, because the velocities of compressional and shear waves are higher in the water-saturated than in the dry state. Kuster and Toksoz (1974) and Toksoz et al (1976) have provided a satisfactory theoretical explanation for this behavior, which is again strongly influenced by the presence of microcracks in the rock.

As part of a number of research studies in the Canadian Shield associated with the stability of underground mine openings (King et al, 1978), seismic reflection surveys (Hajnal et al, 1983), and the proposed use of a tunnel-boring machine (TBM) for developing mine headings, a long-term laboratory rock mechanics program has been conducted to determine the static and dynamic elastic properties of samples of igneous and metamorphic rocks from the Canadian Shield. This paper reports the results of 174 measurements of static elastic modulus (E_s) and 152 measurements of uniaxial compressive strength (C) for these rocks as a function of dynamic elastic modulus (E_D).

EXPERIMENTAL PROCEDURES

Specimen Preparation

The rock samples used in the research program were received in the form of cylindrical pieces of AX-sized core, ranging in diameter from 30 mm to 32.5 mm. After fully saturating with distilled water, first under vacuum and then under a hydrostatic pressure of 10 MPa, cylindrical specimens were cut on a diamond saw and their flat surfaces ground parallel to ± 0.04 mm on a reciprocating grinder. The specimen length-to-diameter ratio lay between 2.0 and 2.3, except for the poorer-quality core when it ranged down to 1.7. The completed test specimens were each weighed in their fully-saturated state and again after vacuum-oven drying at 80°C for 24 hours. At this stage strain gauges were cemented to those specimens for which the stress-strain relations were to be measured with strain gauges. The specimen density and porosity were calculated from the dimensions and weights, dry and saturated; the specimens were then stored and tested in the laboratory environment which lay in the range 20-50% relative humidity and 20-25°C temperature. The specimens tested were all of low porosity, consisting predominantly of crack porosity. In most cases the calculated porosity was less than 1.0%, with the maximum measured value being 1.8%.

Acoustic Velocity Measurements

A block diagram of the test system is shown in Figure 1B. The pulse time-of-flight method for sequentially measuring ultrasonic compressional (P) and shear (S) wave velocities on the same specimen has been described by King (1970). However, a portable ultrasonic non-destructive digital indicating tester (PUNDIT) and combined P- and S-wave transducers, manufactured by C.N.S. Electronics Ltd. (London, U.K.), are now employed for velocity measurements. The rock specimen was mounted between the transmitter and receiver transducer holders, through which it was loaded in uniaxial compression between the platens of a compression testing machine. Lead foil discs 0.04 mm thick were employed to provide acoustic coupling between the rock specimen and transducer holders.

The procedure adopted for velocity measurements was first to load the specimen to an axial stress of 14 MPa in order to bed-in the lead foil. The load was reduced to zero for several minutes, and then P- and S-wave velocity measurements were made an increments of axial stress increasing to 35 MPa. The transducer holders were removed upon conclusion of the velocity measurements, to preserve them from damage during the uniaxial compression tests to failure.

Uniaxial Compression Tests

Static stress-strain relations were measured using either strain gauges with a 12.7 mm gauge length or a re-usable deformation yoke fitted with C-gauge sensors having a 25 mm gauge length. The axial deformation was measured at three positions, separated by a 120° arc, around the specimen. For the compression tests the specimen was placed between a pair of hardened-steel discs of the same diameter as the specimen, with a hemispherical loading seat mounted at the top of the assemblage. The compressive load was applied through the hemispherical seat and steel discs between the platens of the compression testing machine.

The procedure adopted for the uniaxial compression tests was to load the specimen to failure at a constant rate of application of stress of approximately 0.3 MPa/sec. The axial stress and strain during the loading process were recorded either manually or by a data acquisition system, as indicated in Figure 1B.

RESULTS

Data typical of that obtained during the extended series of tests is shown in Figures 1A, 2 and 3. Figure 1A shows the P- and S-wave arrivals, taken from the oscilloscope screen, for a biotite schist (typical of the rock types tested) specimen with little apparent micro-cracking present, subjected to an axial stress of 7 MPa. The velocities calculated for this specimen, following the procedure outlined by King (1970), and also for a second biotite schist specimen with extensive micro-cracking are shown in Figure 2 as a function of axial stress. The degree of microcracking was determined qualitatively from microscopic examination of the specimens, and by the amount of concavity upward observed near the origin of the axial stress-strain curve. The velocities have been corrected for the slight specimen shortening that occurs during uniaxial compression. The accuracy of velocity measurements made in this way is approximately ±0.4%, with a precision of ±0.1% on a given specimen.

The dynamic elastic modulus (E_D) is calculated from the well-known relationship for isotropic materials, involving the compressional (V_p) and shear-wave (V_s) velocities and the rock bulk density (ρ):

$$E_D = \rho V_s^2 \left[\frac{3V_p^2 - 4V_s^2}{V_p^2 - V_s^2} \right]$$

In this paper E_D is reported for an axial stress of 7 MPa, as this was the lowest axial stress for which the shear-wave arrival could be picked unequivocally for the more extensively micro-cracked specimens.

Figure 3 shows the axial stress-strain data obtained for the two biotite schist specimens, one with minor micro-cracking and the second with extensive microcracking. In each case the angle between the schistosity and the specimen axis was approximately 65°. The static elastic modulus (E_s) has been calculated from the linear portion of the stress-strain curve. For a number of rocks, for which the stress-strain curve was found to be concave upwards from the origin for appreciable axial stresses (i.e. the tangent elastic modulus increasing monotonically), the secant values of E_s have been reported over the range of axial stresses from 35MPa to failure.

Figure 4 shows the static elastic modulus (E_s) plotted as a function of the dynamic elastic modulus (E_D) for 174 igneous and metamorphic rock specimens from six sites in the Canadian Shield. Each point plotted represents the average of a number of measurements, for which the latter is indicated in the figure key. Shown in the figure also are E_s and E_D for the two biotite schist specimens referred to above. The hatched area shown in Figure 4 indicates specimens which contained fairly extensive micro-cracking. A linear regression yields the relationship $E_s = 1.263\ E_D - 29.5$, with $r^2 = 0.82$.

Figure 5 shows the uniaxial compressive strength (C) plotted on a log-log scale as a function of dynamic elastic modulus (E_D) for 152 igneous and metamorphic rock specimens from five sites in the Canadian Shield. Again each point plotted represents the mean of a number of measurements, for which the latter is indicated in the figure key. C and E_D for the two biotite schist specimens referred to earlier are also plotted in the figure. The hatched area in the figure indicates specimens which contained fairly extensive micro-cracking. A linear regression yields the relationship $C = 4.31\ (E_D/10)^{1.705}$, with $r^2 = 0.33$.

DISCUSSION

The data plotted in Figure 4 indicate that there is a good correlation between static and dynamic elastic moduli, with the two values converging as the moduli increase in magnitude. It is interesting to note that the relationship determined experimentally here agrees well with that reported by Myung and Helander (1972), for a much smaller number of tests, even though these workers saturated their samples with oil (a weakly-adsorbed liquid) for experiments performed under triaxial test conditions.

The results obtained with rock specimens for which there was an appreciable degree of microfracturing present (generally recovered from the hanging walls of mine stopes, or otherwise damaged during blasting) tend to fall below the linear regression. Specimens of the same rock type, with and without microfracturing present, were observed to exhibit the same behavior as that shown in Figure 4 for the two biotite schist specimens: the progression from minor to extensive microcracking tends in the plot to lie approximately parallel to the linear regression.

The data plotted in Figure 5 indicate that the correlation between compressive strength and dynamic elastic modulus is not nearly as good as that of the static elastic modulus. There are two reasons probably for this behavior. The first is that the compressive strength is sensitive to the orientation and pervasiveness of the microfracturing existing in the rock. The second reason is probably similar to that reported by Colback and Wiid (1965): that there is a scatter in compressive strength values because the latter are particularly sensitive to the moisture content of the environment in which the rock specimens are tested. This is more so than is the case with the dynamic elastic modulus, which is a function of the compressional and shear-wave velocities, in the range of relative humidities (20 to 50 percent) reported for these experiments (see, for instance, Pandit and King, 1979 and Clark et al, 1980). Colback and Wiid measured a reduction in uniaxial compressive strength of approximately 20 percent for a quartzitic sandstone when the relative humidity of the test environment was increased from 15 to 45 percent, whereas the reduction in dynamic elastic modulus for a sandstone over the same change in relative humidity found by Pandit and King was approximately 12 percent. Although these rocks are not typical of those crystalline rocks tested in the research reported here, similar behavior has been observed for crystalline rocks.

It is clear that if valid correlations are to be established, the environment in which the rocks specimens are stored and the experimental tests are performed must be carefully controlled. This is particularly true if a correlation between strength and an elastic property is to be established.

ACKNOWLEDGMENTS

Provision of rock samples and some financial support from the following mining companies is gratefully acknowledged: Sherritt-Gordon Mines, Hudson Bay Mining and Smelting Company, and the International Nickel Company. Operating grants from the Defense Research Board of Canada and the National Research Council of Canada are also gratefully acknowledged for major support of the research reported.

The publication was prepared under Department of Energy Contract No. DE-AC03-76SF00098 with Lawrence Berkeley Laboratory.

REFERENCES

Boozer, G.D., Hiller, K.H., and Serdengecti, S. Effects of pore fluids on the deformation behavior of rocks subjected to triaxial compression. Proceedings 5th U.S. Rock Mechanics Symposium, Minneapolis, pp. 579-625 (1963).

Clark, V.S., Tittman, B.R., and Spencer, T.W. Effect of volatiles on attenuation (Q^{-1}) and velocity in sedimentary rocks. Journal of Geophysical Research, v. 85, pp. 5190-5198 (1980).

Colback, P.S.B. and Wiid, B.L. The influence of moisture content on the compressive strength of rocks. Proceedings of 3rd Canadian Rock Mechanics Symposium, Toronto, pp. 65-83, Information Canada: Ottawa (1965).

Geyer, R.L. and Myung, J.I. The 3-D velocity log: a tool for in-situ determination of the elastic moduli of rocks. Proceedings 12th U.S. Symposium on Rock Mechanics, Rolla, pp. 71-107 (1971).

Gladwin, M.T. Ultrasonic stress monitoring in underground mining. Internat. Journ. Rock Mechanics and Mining Sciences, v. 19, pp. 221-228 (1982).

Gladwin, M.T. and Stacey, F.D. Ultrasonic pulse velocity as a rock stress sensor. Tectonophysics, v. 21, pp. 39-45 (1974).

Hajnal, Z., Stauffer, M.R., King, M.S., Wallis, P.F., Wang, H.F., and Jones, L. Seismic characteristics of a Precambrian pluton and its adjacent rocks. Geophysics, v. 48, in press (1983).

King, M.S. Static and dynamic elastic moduli of rocks under pressure. Procedings 11th U.S. Symposium on Rock Mechanics, Berkeley, pp. 329-351 (1970).

King, M.S., Stauffer, M.R., and Pandit, B.I. Quality of rock masses by acoustic borehole logging. Proceedings 3rd Internat. Congress IAEG, Madrid, Sect. IV, v. 1, pp. 156-164 (1978).

Kuster, G.T. and Toksoz, M.N. Velocity and attenuation of seismic waves in two-phase media: Part I. Theoretical formulations. Geophysics, v. 39, pp. 587-606 (1974).

McCann, D.M., Grainger, P. and McCann, C. Inter-borehole acoustic measurements and their use in engineering geology. Geophysical Prospecting, v. 23, pp. 50-69 (1975).

McKenzie, C.K., Stacey, G.P., and Gladwin, M.T. Ultrasonic characteristics of a rock mass. Internat. Journ. Rock Mechanics and Mining Sciences, v. 19, pp. 25-30 (1982).

Myung, J.I. and Helander, D.P. Correlation of elastic moduli dynamically measured by in-situ and laboratory techniques. Proceedings 13th Annual Logging Symposium of SPWLA, Tulsa, p. H1-H25 (1972).

Pandit, B.I. and King, M.S. The variation of elastic wave velocities and quality factor Q of a sandstone with moisture content. Canadian Journ. of Earth Sciences, v. 16, pp. 2187-2195 (1979).

Paulsson, B.N.P. and King, M.S. Between-hole acoustic surveying and monitoring of a granitic rock mass. Internat. Journ. Rock Mechanics and Mining Sciences, v. 17, pp. 371-376 (1980a).

Paulsson, B.N.P. and King, M.S. A cross-hole investigation of a rock mass subjected to heating. Proceedings Internat. Symposium on Subsurface Space: Rockstore 80, v. 2, pp. 969-976 (1980b).

Simmons, G. and Brace, W.F. Comparison of static and dynamic measurements of compressibility of rocks. Journ. Geophysical Research, v. 70, pp. 5649-5656 (1965).

Sjogren, G., Ofsthus, A., and Sandberg, J. Seismic classification of rock mass qualities. Geophysical Prospecting, v. 27, pp. 409-442 (1979).

Toksoz, M.N., Cheng, C.H., and Timur, A. Velocities of seismic waves in porous rocks. Geophysics, v. 41, pp. 621-645 (1976).

West, G. and New, B.M. An ultrasonic velocity borehole logger for use in rock. Ultrasonics, v. 19, pp. 67-71 (1981).

FIGURE CAPTIONS

Figure 1. (a) Compressional and shear-wave arrivals for biotite schist.
(b) Block diagram of equipment.

Figure 2. Ultrasonic compressional and shear-wave velocities for two biotite schist specimens as a function of axial stress. E_D is the dynamic elastic modulus.

Figure 3. Axial stress as a function of axial strain for two biotite schist specimens. E_S is the static elastic modulus and C the compressive strength.

Figure 4. Static elastic modulus as a function of dynamic elastic modulus for 174 igneous and metamorphic rock specimens.

Figure 5. Uniaxial compressive strength as a function of dynamic elastic modulus for 152 igneous and metamorphic rock specimens.

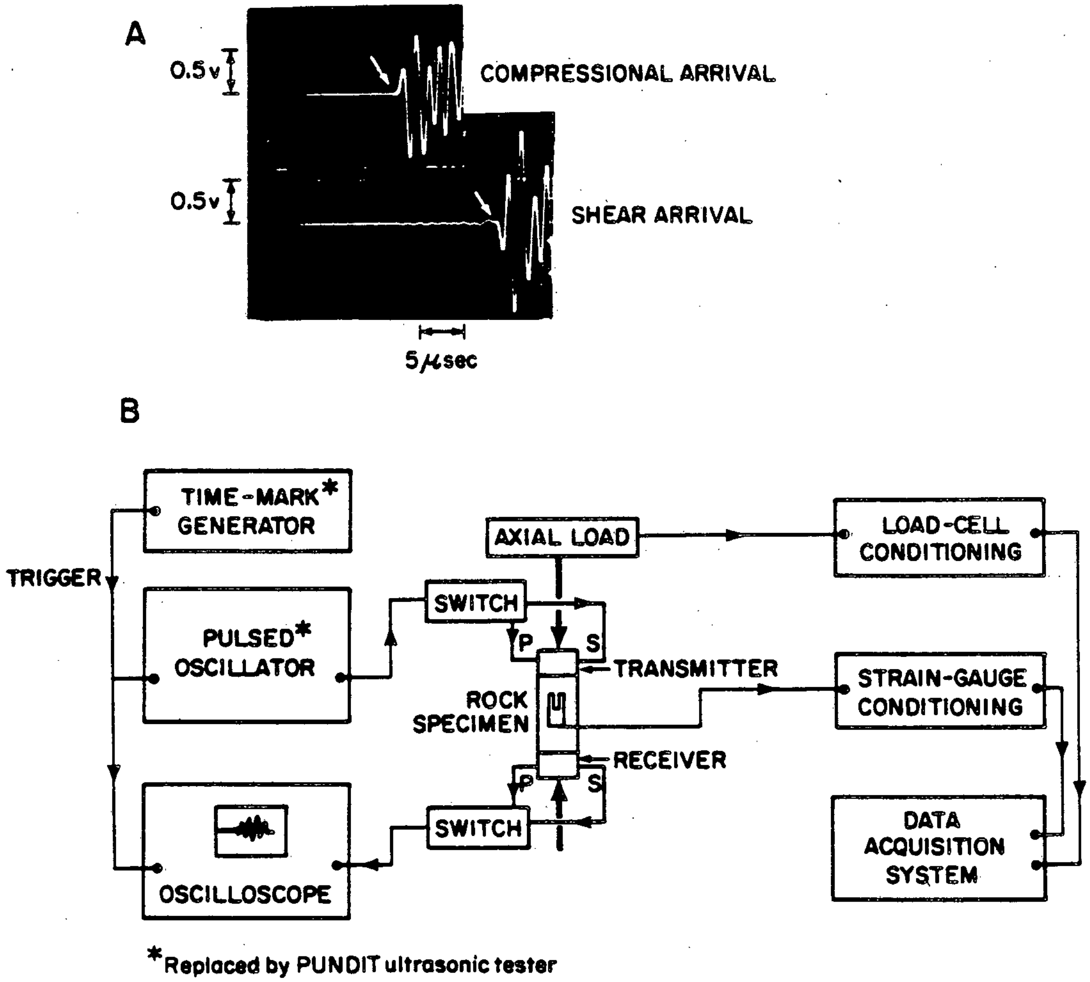
A
0.5v
COMPRESSIONAL ARRIVAL
0.5v
SHEAR ARRIVAL
5μsec
B
TIME-MARK*
GENERATOR
TRIGGER
PULSED*
OSCILLATOR
OSCILLOSCOPE
SWITCH
SWITCH
AXIAL LOAD
P
S
TRANSMITTER
ROCK
SPECIMEN
RECEIVER
P
S
LOAD-CELL
CONDITIONING
STRAIN-GAUGE
CONDITIONING
DATA
ACQUISITION
SYSTEM
*Replaced by PUNDIT ultrasonic tester

Fig.1

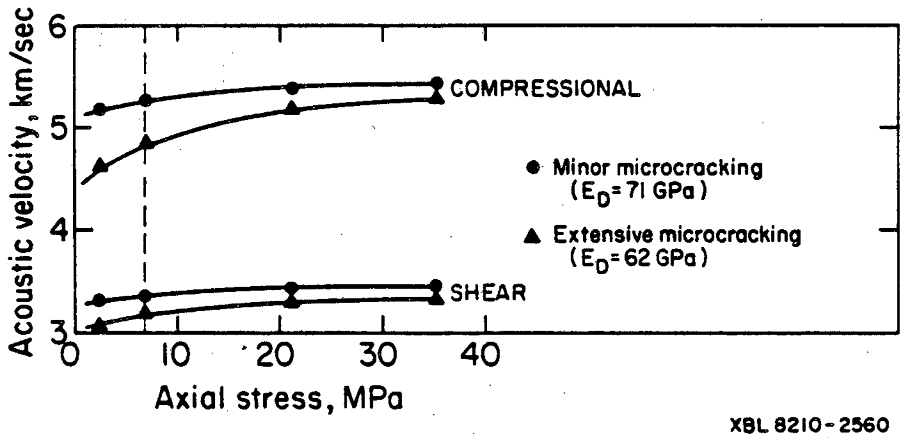
COMPRESSIONAL
SHEAR
Minor microcracking
(E_D= 71 GPa)
Extensive microcracking
(E_D= 62 GPa)
Acoustic velocity, km/sec
Axial stress, MPa
6
5
4
3
0
10
20
30
40
XBL 8210-2560

Fig. 2

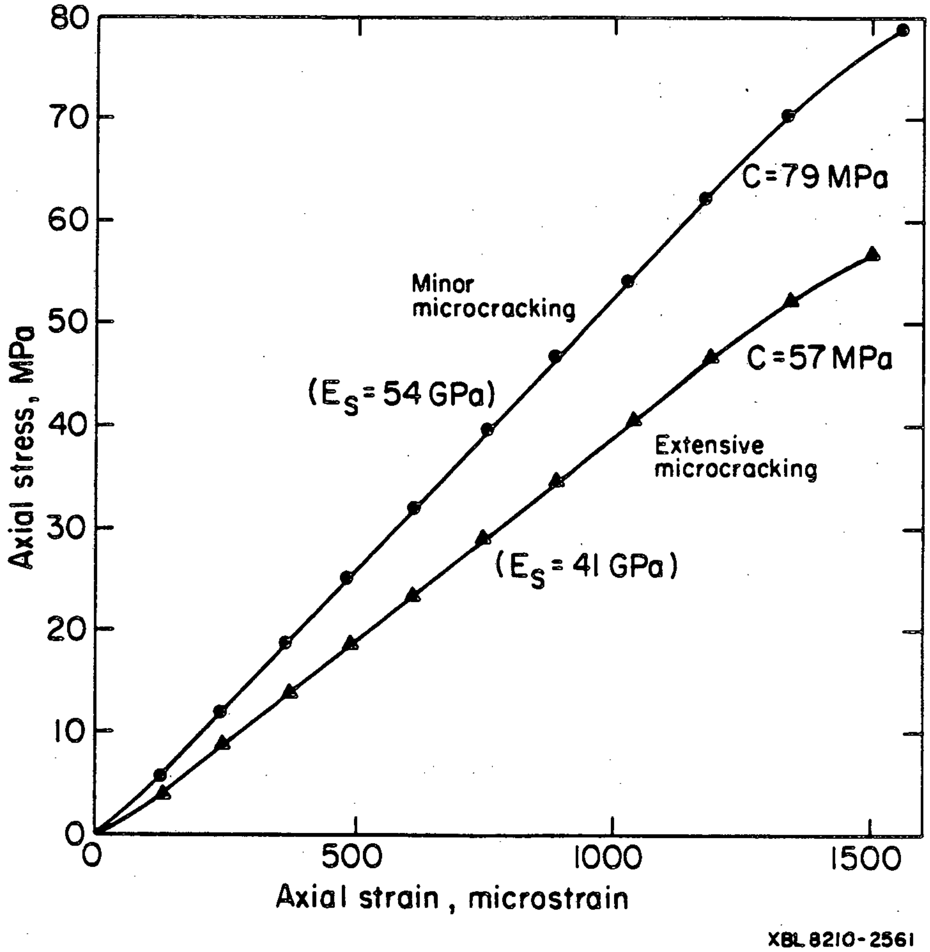

80
70
60
50
40
30
20
10
0
0
500
1000
1500
Axial stress, MPa
Axial strain, microstrain
C=79 MPa
Minor microcracking
(E$_S$=54 GPa)
C=57 MPa
Extensive microcracking
(E$_S$=41 GPa)
XBL 8210-2561

Fig. 3

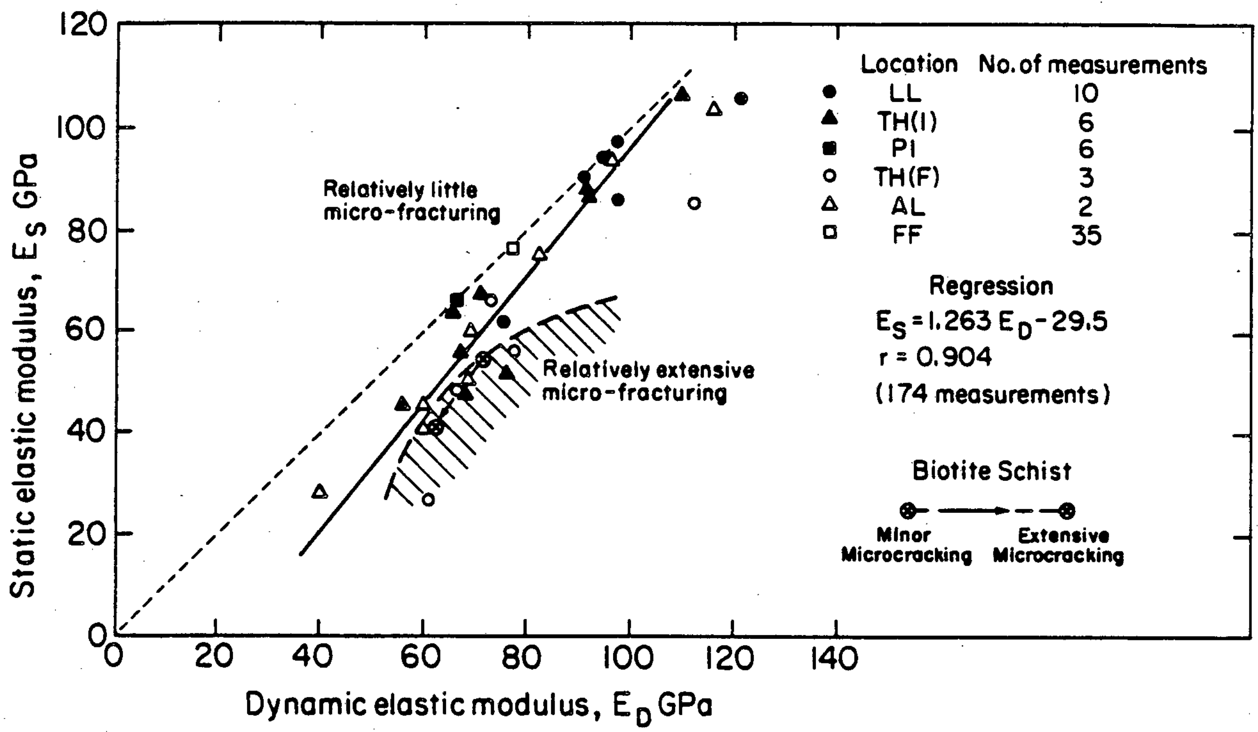

XBL 8210-2559

Fig.4

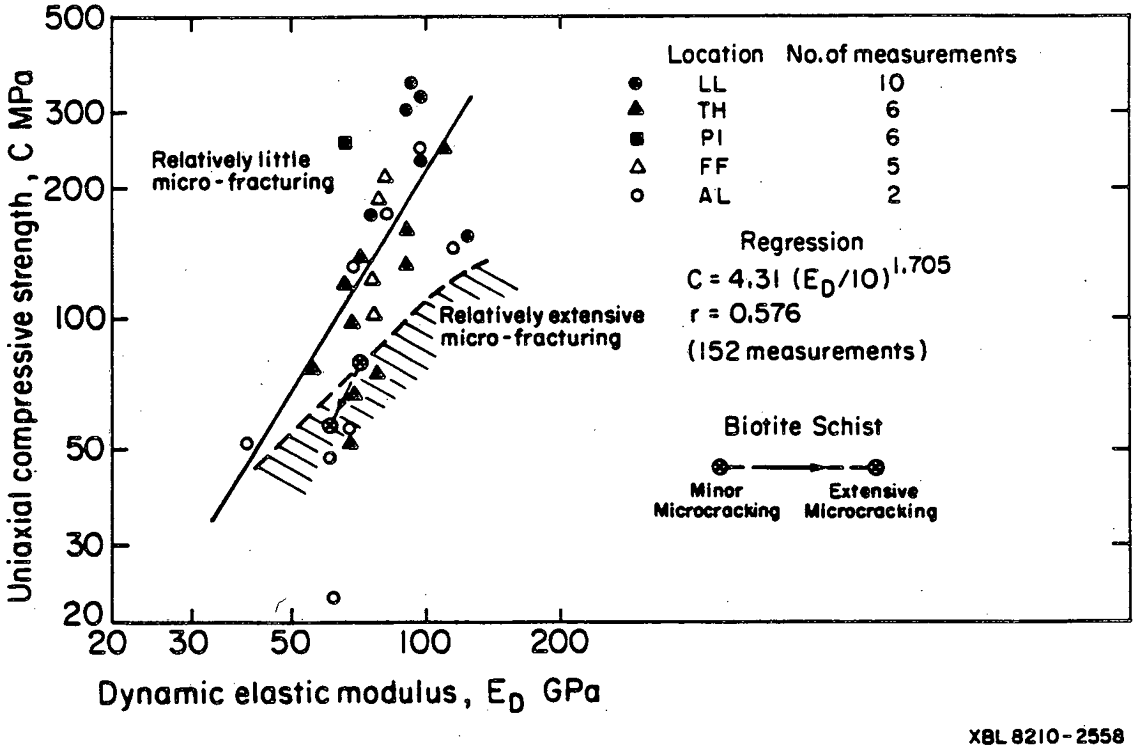
500
300
200
100
50
30
20
20
30
50
100
200
Uniaxial compressive strength, C MPa
Dynamic elastic modulus, E_D GPa
Relatively little micro-fracturing
Relatively extensive micro-fracturing
Location No. of measurements
LL 10
TH 6
PI 6
FF 5
AL 2
Regression
$C = 4.31 (E_D/10)^{1.705}$
r = 0.576
(152 measurements)
Biotite Schist
Minor Microcracking
Extensive Microcracking
XBL 8210-2558

Fig. 5

TECHNICAL INFORMATION DEPARTMENT
LAWRENCE BERKELEY LABORATORY
UNIVERSITY OF CALIFORNIA
BERKELEY, CALIFORNIA 94720